

# Noble-Metal-Free Deoxygenation of Epoxides: Titanium Dioxide as a Photocatalytically Regenerable Electron-Transfer Catalyst

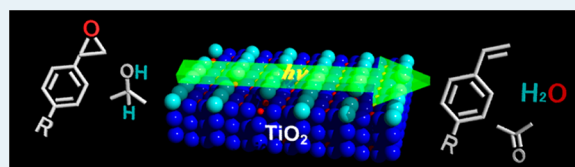
Yasuhiro Shiraishi,\* Hiroaki Hirakawa, Yoshiki Togawa, and Takayuki Hirai

Research Center for Solar Energy Chemistry, and Division of Chemical Engineering, Graduate School of Engineering Science, Osaka University, Toyonaka 560-8531, Japan

## Supporting Information

**ABSTRACT:** Catalytic deoxygenation of epoxides into the corresponding alkenes is a very important reaction in organic synthesis. Early reported systems, however, require noble metals, high reaction temperatures (>373 K), or toxic reducing agents. Here, we report a noble-metal-free heterogeneous catalytic system driven with alcohol as a reducing agent at room temperature. Photoirradiation ( $\lambda < 420$  nm) of semiconductor titanium dioxide ( $\text{TiO}_2$ ) with alcohol promotes efficient and selective deoxygenation of epoxides into alkenes. This noble-metal-free catalytic deoxygenation is facilitated by the combination of electron transfer from surface  $\text{Ti}^{3+}$  atoms on  $\text{TiO}_2$  to epoxides, which promotes deoxygenation of epoxides, and photocatalytic action of  $\text{TiO}_2$ , which regenerates oxidized surface Ti atoms with alcohol as a reducing agent.

**KEYWORDS:** photocatalysis, titanium dioxide, surface defects, reduction, deoxygenation



## INTRODUCTION

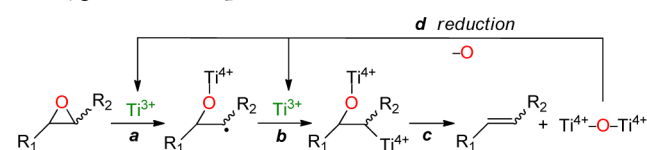
Deoxygenation of epoxides into the corresponding alkenes is an essential reaction in biological systems for the reproduction of vitamin K in the vitamin K cycle.<sup>1,2</sup> Deoxygenation is also a very important reaction in organic synthesis for the deprotection of the oxirane ring, a protecting group for C=C bonds.<sup>3–5</sup> The reaction is usually carried out using a stoichiometric or excess amount of toxic reducing agents, such as phosphines, silanes, iodides, and heavy metals, with a concomitant formation of copious amount of wastes.<sup>6</sup> Catalytic deoxygenation driven by easily recyclable heterogeneous catalyst is therefore an ideal process. Several heterogeneous systems have been proposed so far for catalytic deoxygenation of epoxides.<sup>7–13</sup> These systems employ gold or silver nanoparticles loaded on metal oxide supports with molecular hydrogen ( $\text{H}_2$ ), carbon monoxide (CO), or alcohol as a reducing agent. They successfully promote selective deoxygenation at the reaction temperatures ranging from room temperature to 353 K, but require noble metals as the catalyst. An alternative process, which promotes efficient and selective deoxygenation with a noble-metal-free heterogeneous catalyst, is necessary for green organic synthesis.

Very recently, Li et al.<sup>14</sup> reported that UV irradiation of semiconductor titanium dioxide ( $\text{TiO}_2$ ) in alcohol with epoxides successfully produces the corresponding alkenes. The reaction proceeds without noble metals at room temperature; therefore, it is a potential green catalytic system for deoxygenation. They proposed that the deoxygenation proceeds via the two-electron reduction of epoxide by the conduction band electrons ( $e^-$ ) on the photoactivated  $\text{TiO}_2$ . The reduction potential of epoxide (e.g., styrene oxide) is, however,  $-2.4$  V (vs NHE, pH 0),<sup>12</sup> which is significantly more negative than the bottom of the  $\text{TiO}_2$  conduction band ( $\sim 0$

V).<sup>15</sup> This means that two-electron reduction of epoxides by the conduction band  $e^-$  is thermodynamically unfavorable. Detailed study on the deoxygenation mechanism is therefore necessary.

It is well-known that trivalent titanium atom ( $\text{Ti}^{3+}$ ) behaves as a single-electron-transfer reagent, as often reported for titanocene complexes.<sup>16,17</sup> As shown in Scheme 1, the  $\text{Ti}^{3+}$

## Scheme 1. Catalytic Cycle for Titanocene-Promoted Deoxygenation of Epoxides



atom within a titanocene complex<sup>18</sup> promotes a homolytic cleavage of the oxirane ring via the single-electron-transfer to the oxygen atom (a).<sup>19</sup> The radical formed is reduced by the reaction with the other  $\text{Ti}^{3+}$  atom (b).<sup>20</sup>  $\beta$ -Elimination of the intermediate produces the corresponding alkenes with a formation of oxidized two Ti atoms (c). These reactions proceed efficiently and selectively even at room temperature, although the system suffers from the reduction step for oxidized Ti atoms (d); regeneration of  $\text{Ti}^{3+}$  requires hazardous reducing agents, such as silanes and heavy metals.<sup>21</sup>

In the present work, we clarified the mechanism for deoxygenation of epoxides on the photoactivated  $\text{TiO}_2$  by

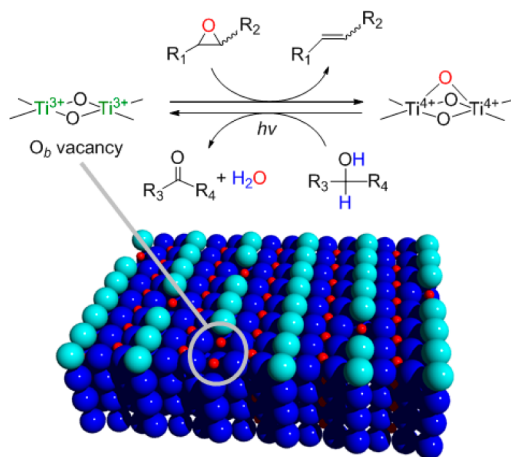
Received: January 17, 2014

Revised: April 15, 2014

Published: April 16, 2014

means of X-ray photoelectron spectroscopy (XPS) and diffuse-reflectance infrared Fourier transform (DRIFT) analysis. The active sites for deoxygenation are the  $\text{Ti}^{3+}$  atoms located at the surface defects. As shown in Scheme 2, the  $\text{TiO}_2$  (110) surface

**Scheme 2. Catalytic Cycle for Deoxygenation of Epoxides on the Surface of  $\text{TiO}_2$  (110) under Photoirradiation<sup>a</sup>**



<sup>a</sup>The light blue spheres that lie in the (001) azimuth are the  $\text{O}_b$  atoms, and the parallel red spheres are the Ti atoms, respectively.

is characterized by alternate rows of 5-fold-coordinated  $\text{Ti}^{4+}$  atoms and bridging O atoms ( $\text{O}_b$ ) that run in the (001) direction.<sup>22</sup> Surface defects are the  $\text{O}_b$  vacancies, where two excess electrons associated with  $\text{O}_b$  are transferred to the empty 3d orbitals of neighboring  $\text{Ti}^{4+}$  atoms, producing two exposed  $\text{Ti}^{3+}$  atoms.<sup>23</sup> These  $\text{Ti}^{3+}$  atoms promote deoxygenation of epoxides via the single electron transfers, producing alkenes and oxidized Ti atoms. In contrast, photoexcitation of  $\text{TiO}_2$  produces electron ( $\text{e}^-$ ) and positive hole ( $\text{h}^+$ ) pairs.<sup>24–27</sup> The  $\text{e}^-$ 's reduce the oxidized Ti atoms, and the  $\text{h}^+$ 's oxidize alcohol.

This photocatalytic cycle successfully regenerates the surface  $\text{Ti}^{3+}$  atoms with alcohol as a reducing agent, thus promoting efficient catalytic deoxygenation.

## RESULTS AND DISCUSSION

Deoxygenation of styrene oxide was carried out with 2-PrOH in the presence of  $\text{TiO}_2$  particles with different surface areas. Table 1 summarizes the results obtained by photoirradiation ( $\lambda > 300$  nm, 6 h) of  $\text{TiO}_2$  (10 mg) in a 2-PrOH/MeCN mixture (5/5 v/v, 5 mL) with styrene oxide (20 mM) under  $\text{N}_2$  atmosphere. All of the  $\text{TiO}_2$  particles (samples 1–9) produce styrene with very high selectivity (84–95%), although the styrene yields are different from each other. GC analysis of the solutions recovered after the reaction detected minor amounts of 2-phenylethanol as a byproduct. IR analysis of the solution (Figure S2, Supporting Information) showed a band at  $\sim 1110$   $\text{cm}^{-1}$  assigned to C–O stretching of the ether linkage, suggesting that polymerized styrene oxide is also involved as a byproduct, as observed in related catalytic systems.<sup>28</sup> As shown in Table 1 (sample 10), the dark reaction scarcely promotes deoxygenation. In addition, photoirradiation without alcohol (sample 11) also does not promote reaction. These data indicate that photoirradiation with alcohol is necessary for deoxygenation.

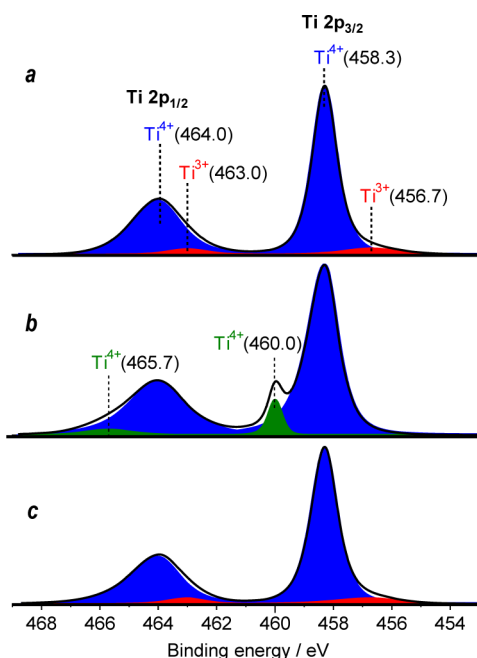
The active sites for deoxygenation of epoxide are the surface  $\text{Ti}^{3+}$  atoms on  $\text{TiO}_2$  (Scheme 2). XPS analysis confirms this. As shown in Figure 1a, XPS chart for  $\text{TiO}_2$  (sample 9) shows Ti  $2p_{1/2}$  and  $2p_{3/2}$  signals, both of which consist of bulk  $\text{Ti}^{4+}$  (blue) and surface  $\text{Ti}^{3+}$  (red) atoms.<sup>29</sup> In contrast, as shown in Figure 1b, adsorption of styrene oxide onto  $\text{TiO}_2$  in the gas phase leads to complete disappearance of the surface  $\text{Ti}^{3+}$  signal (red), along with a formation of new  $\text{Ti}^{4+}$  signal at a higher binding energy (green). This clearly indicates that the surface  $\text{Ti}^{3+}$  atoms are oxidized to  $\text{Ti}^{4+}$ <sup>30</sup> via electron transfer to styrene oxide.

The electron transfer from the surface  $\text{Ti}^{3+}$  atoms promotes deoxygenation of epoxide. This is confirmed by DRIFT analysis

**Table 1. Deoxygenation of Styrene Oxide on Various  $\text{TiO}_2$  Particles under Photoirradiation<sup>a</sup>**

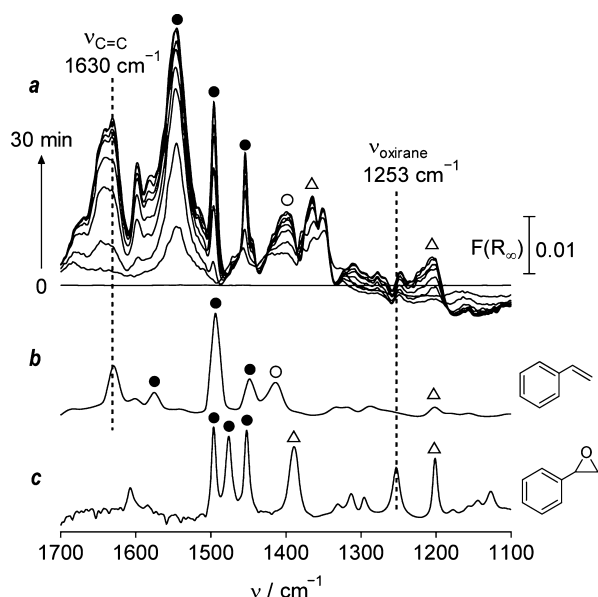
sample	catalyst	crystalline phase <sup>b</sup>	BET surface area ( $\text{m}^2 \text{g}^{-1}$ ) <sup>c</sup>	styrene oxide conv. (%) <sup>d</sup>	styrene yield (%) <sup>d</sup>	select. (%)	$N_{\text{Ti}}$ ( $\mu\text{mol g}^{-1}$ ) <sup>e</sup>	$v_i$ ( $\mu\text{mol h}^{-1}$ ) <sup>f</sup>
1	ST-41 <sup>g</sup>	A	8	10	9	84	2.9	1.4
2	ST-21 <sup>g</sup>	A	11	44	38	86	34.2	6.1
3	Aldrich anatase	A	67	43	36	84	12.8	5.7
4	ST-01 <sup>g</sup>	A	217	62	54	87	59.4	10.0
5	P25 <sup>h</sup>	A/R (83/17)	59	94	85	88		
6	NS-51 <sup>i</sup>	R	7	49	41	84	15.9	7.7
7	Wako rutile	R	15	<1	<1		1.9	<1
8	PT-101 <sup>g</sup>	R	25	77	69	90	81.6	11.4
9	JRC-TIO-6 <sup>h</sup>	R	100	>99	95	95	168.0	25.7
10 <sup>j</sup>	JRC-TIO-6			<1	<1			
11 <sup>k</sup>	JRC-TIO-6			<1	<1			

<sup>a</sup>Photoirradiation was carried out using a 2 kW Xe lamp (light intensity at 300–450 nm is  $27.3 \text{ W m}^{-2}$ ). <sup>b</sup>Determined by X-ray diffraction (XRD) analysis (Figure S1, Supporting Information). <sup>c</sup>Determined by  $\text{N}_2$  adsorption/desorption analysis (ref 37). <sup>d</sup>Determined by GC analysis. <sup>e</sup>The number of surface  $\text{Ti}^{3+}$  atoms per gram  $\text{TiO}_2$ , measured by DRIFT analysis of nitrobenzene adsorbed on  $\text{TiO}_2$  in the gas phase (Figure S3, Supporting Information). <sup>f</sup>Initial rate for styrene formation during 3 h photoreaction. <sup>g</sup>Supplied from Ishihara Sangyo, Ltd. (Japan). <sup>h</sup>Japan Reference Catalyst supplied from the Catalyst Society of Japan. <sup>i</sup>Supplied from Toho Titanium Co., Ltd. (Japan). <sup>j</sup>Reaction was performed in the dark. <sup>k</sup>Reaction was performed in MeCN without 2-PrOH.



**Figure 1.** XPS chart in the Ti 2p region of (a) TiO<sub>2</sub> (sample 9), (b) the sample after adsorption of styrene oxide in the gas phase, and (c) the sample after photoirradiation ( $\lambda > 300$  nm) in 2-PrOH for 6 h.

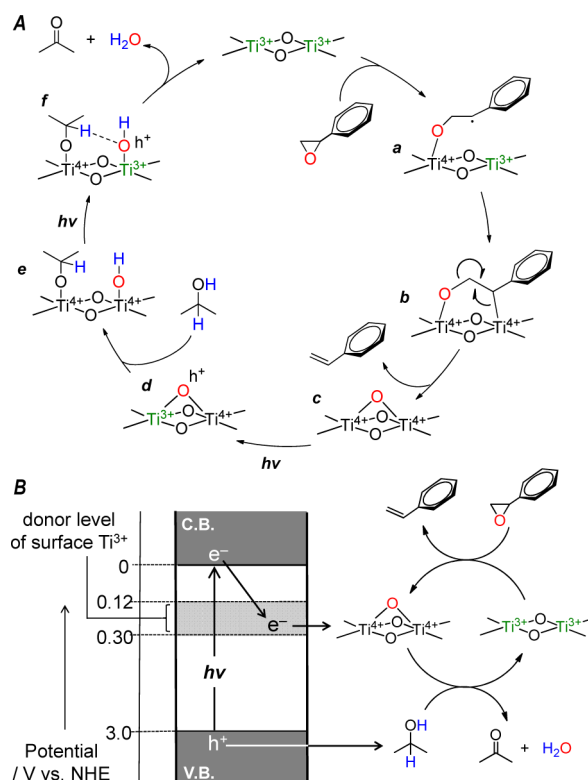
of styrene oxide adsorbed onto TiO<sub>2</sub> (sample 9) in the gas phase. Figure 2a shows the time-dependent change in the spectrum after the injection of styrene oxide. A distinctive absorption band appears at 1630 cm<sup>-1</sup>, which is assigned to the C=C stretching vibration ( $\nu_{C=C}$ ) of the styrene formed,<sup>31,32</sup> as evidenced by the spectrum of styrene (Figure 2b). In this case, a band assigned to the breathing mode of oxirane ring



**Figure 2.** (a) Time-dependent change in the DRIFT spectra of styrene oxide adsorbed onto TiO<sub>2</sub> (sample 9) in the gas phase at 303 K. Attenuated total reflection (ATR) spectra of (b) styrene and (c) styrene oxide measured at 303 K. The absorption bands indicated by ●, ○, and △ are assigned to phenyl ring stretching, =CH<sub>2</sub> deformation, and phenyl C–H stretching (refs 31 and 32), respectively.

( $\nu_{\text{oxirane}}$ ),<sup>33</sup> observed for styrene oxide at  $\sim 1250$  cm<sup>-1</sup> (Figure 2c), scarcely appears. The results clearly indicate that styrene oxide adsorbed onto the TiO<sub>2</sub> surface is immediately transformed to styrene via the electron transfer from the surface Ti<sup>3+</sup> atoms under dark condition. The catalytic mechanism for deoxygenation of epoxide by surface Ti<sup>3+</sup> atoms can therefore be summarized as Scheme 3A. One Ti<sup>3+</sup>

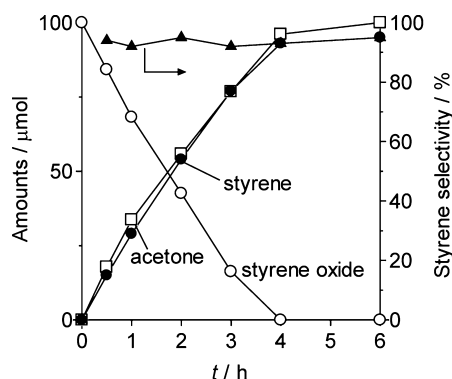
**Scheme 3. (A) Proposed Mechanism for Epoxide Deoxygenation on TiO<sub>2</sub> Surface with Alcohol under Photoirradiation, and (B) Energy Diagram for Regeneration of Surface Ti<sup>3+</sup> by Photoexcitation of TiO<sub>2</sub>**



atom promotes homolytic cleavage of the oxirane ring via the Ti<sup>4+</sup>–O bond formation (a). The radical formed is reduced by another Ti<sup>3+</sup> and produces a bridged intermediate (b). β-Elimination of the intermediate affords the corresponding alkene, along with a formation of oxidized two Ti<sup>4+</sup> atoms (c).

The surface Ti atoms oxidized by deoxygenation of epoxide (Scheme 3A.c) are reduced by the conduction band e<sup>-</sup> produced by photoexcitation of TiO<sub>2</sub> with alcohol as the reducing agent (d–f).<sup>34</sup> This regenerates the surface Ti<sup>3+</sup> atoms and completes the catalytic cycle. XPS analysis confirms this. As shown in Figure 1b, TiO<sub>2</sub> after adsorption of styrene oxide exhibits green signals assigned to the oxidized surface Ti atoms. However, as shown in Figure 1c, the TiO<sub>2</sub> sample, when photoirradiated in 2-PrOH under N<sub>2</sub> atmosphere, leads to disappearance of the green signals, along with a regeneration of Ti<sup>3+</sup> signals (red), similar to those observed for pure TiO<sub>2</sub> (Figure 1a). This indicates that, as shown in Scheme 3A.d–f, the oxidized surface Ti atoms are reduced to Ti<sup>3+</sup> by photoirradiation with alcohol.

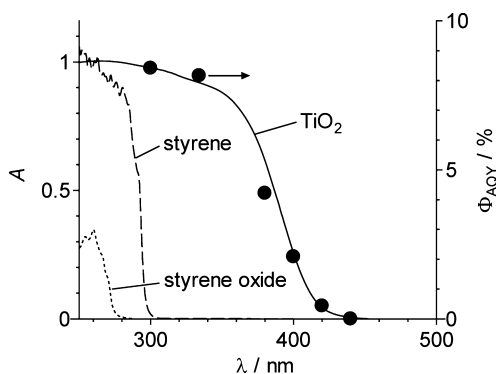
Figure 3 shows the time-dependent change in the amounts of substrate and products during the reaction of styrene oxide in a 2-PrOH solution with TiO<sub>2</sub> (sample 9) under photoirradiation. Reaction for 4 h leads to complete conversion of styrene oxide



**Figure 3.** Time-dependent change in the amounts of substrate and products during photoreaction of styrene oxide with  $\text{TiO}_2$  (sample 9) in a 2-PrOH solution. Conditions are identical to those in Table 1.

to styrene ( $100 \mu\text{mol}$ ) with a formation of an almost equivalent amount of acetone ( $100 \mu\text{mol}$ ). GC analysis also detected the formation of water. These data suggest that, as shown in Scheme 3A.d–f, photoirradiation reduces the oxidized surface Ti atoms with alcohol as the reducing agent, and the H atoms of alcohol are removed as water.

The oxidized surface Ti atoms are reduced by photoexcitation of  $\text{TiO}_2$ . Action spectrum analysis confirms this. Figure 4 shows the apparent quantum yield for styrene

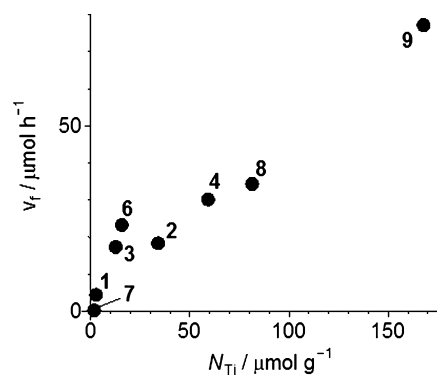


**Figure 4.** (line) Absorption spectra of  $\text{TiO}_2$  (sample 9), styrene oxide, and styrene. (black circle) Action spectrum for styrene formation obtained by the photoreaction of styrene oxide on the catalyst. The apparent quantum yield for styrene formation was determined using the equation  $\Phi_{\text{AQY}} (\%) = (\text{styrene formed} \times 2) / (\text{photon number entering into the reaction vessel}) \times 100$  (see the Experimental Section).

formation ( $\Phi_{\text{AQY}}$ ), obtained by photoreaction of styrene oxide with  $\text{TiO}_2$  (sample 9) using the monochromatic lights. The quantum yields are consistent with the absorption spectrum of  $\text{TiO}_2$ , suggesting that the regeneration of surface  $\text{Ti}^{3+}$  is promoted by band gap excitation of  $\text{TiO}_2$ . As shown in Scheme 3B, the edges of the conduction band ( $E_{\text{CB}}$ ) and valence band ( $E_{\text{VB}}$ ) of  $\text{TiO}_2$  (rutile) are located at 0 and 3.0 V (vs NHE, pH 0),<sup>15</sup> respectively. In contrast, the donor levels of surface  $\text{Ti}^{3+}$  atoms are located at 0.12–0.3 eV below  $E_{\text{CB}}$ .<sup>35</sup> As a result of this, band gap excitation of  $\text{TiO}_2$  and subsequent trapping of the conduction band  $e^-$  by the oxidized Ti atoms<sup>36</sup> regenerate surface  $\text{Ti}^{3+}$  atoms, while the positive hole ( $h^+$ ) formed on  $\text{TiO}_2$  oxidizes alcohol. This photocatalytic cycle (Scheme 3B) allows successful regeneration of surface  $\text{Ti}^{3+}$

atoms with alcohol, thereby promoting efficient deoxygenation of epoxides.

The surface  $\text{Ti}^{3+}$  atoms on  $\text{TiO}_2$  behave as active sites for deoxygenation; therefore, the number of surface  $\text{Ti}^{3+}$  atoms ( $N_{\text{Ti}}$ ) critically affects the deoxygenation activity. The  $N_{\text{Ti}}$  values can be determined by DRIFT analysis of nitrobenzene adsorbed onto the  $\text{TiO}_2$  surface in the gas phase;<sup>37,38</sup> as shown in Figure S3 (Supporting Information), the intensity of symmetric vibrational band ( $1346 \text{ cm}^{-1}$ ) assigned to the nitrobenzene adsorbed onto the surface  $\text{Ti}^{3+}$  atoms allows accurate determination of  $N_{\text{Ti}}$ . The  $N_{\text{Ti}}$  ( $\mu\text{mol g}^{-1}$ ) values for the respective  $\text{TiO}_2$ 's are summarized in Table 1, and Figure 5



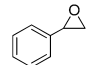
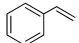
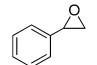
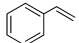
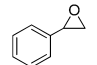
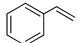
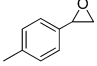
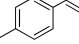
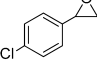
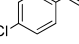
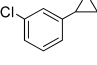
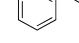
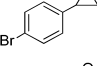
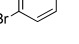
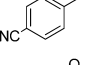
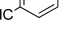
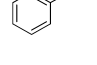
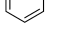
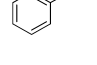
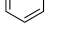
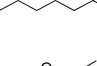

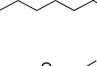

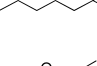

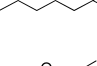

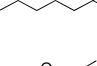

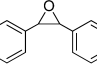
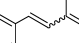
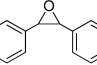
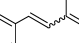
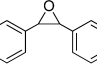
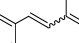
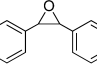
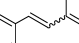
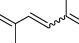
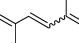
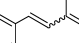
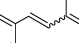
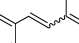
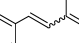
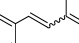
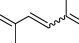
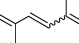
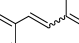
**Figure 5.** Relationship between the number of surface  $\text{Ti}^{3+}$  atoms ( $N_{\text{Ti}}$ ) and the average initial rate for styrene formation ( $v_f$ ) during photoreaction (3 h) of styrene oxide on the respective  $\text{TiO}_2$ . The sample numbers correspond to those listed in Table 1.

shows the relationship between  $N_{\text{Ti}}$  and the average initial rate for styrene formation ( $v_f/\mu\text{mol h}^{-1}$ ) on the respective  $\text{TiO}_2$  determined by 3 h photoreaction. The proportional relationship between  $N_{\text{Ti}}$  and  $v_f$  suggests that surface  $\text{Ti}^{3+}$  atoms indeed behave as the deoxygenation sites, and the  $\text{TiO}_2$  particles with a larger number of surface  $\text{Ti}^{3+}$  is effective for deoxygenation.

The reaction scope of this  $\text{TiO}_2$  system is summarized in Table 2. Photoirradiation of  $\text{TiO}_2$  (sample 9) in a 2-PrOH solution promotes deoxygenation of various kinds of epoxides into alkenes. For example, styrene oxides with several types of substituents are successfully converted to styrenes (entries 1–9). In particular, the reducible substituents such as halogen and cyano groups are retained unchanged during deoxygenation (entries 5–8). In addition, as shown in entries 2 and 3, the  $\text{TiO}_2$  catalyst recovered after photoreaction of styrene oxide (entry 1), when reused for further reaction, exhibits almost the same yields of styrene. This indicates that the catalyst is reusable without any loss of activity and selectivity.

In contrast, as shown by entries 10 and 12, aliphatic epoxides such as 1,2-epoxyoctane and glycidyl phenyl ether show low yields of alkenes (31 and 41%), although the selectivities are high (82 and 88%). This is due to the low efficiency for electron transfer from  $\text{Ti}^{3+}$  to the oxygen atom of their oxirane ring, suppressing their ring-opening (Scheme 3a). As shown in Figure S4 (Supporting Information), ab initio calculation based on the density functional theory (DFT) revealed that the electron density of the oxygen atom for LUMO of the aliphatic epoxides is significantly smaller than that of aromatic epoxides.<sup>39</sup> This suggests that it is difficult for the electron to transfer from  $\text{Ti}^{3+}$  to the oxygen atoms of aliphatic epoxide. Figure 6a shows the DRIFT spectra of 1,2-epoxyoctane adsorbed onto the surface of  $\text{TiO}_2$  (sample 9) in the gas

Table 2. Deoxygenation of Various Epoxides on TiO<sub>2</sub> under Photoirradiation<sup>a</sup>

Entry	Substrate	<i>t</i> [h]	Temp. [K]	Light irradiated [nm]	Product	Yield [%] <sup>b</sup>	Selectivity [%]
1						95	95
2 <sup>c</sup>		6	303	>300		93	93
3 <sup>d</sup>						95	95
4		6	303	>300		94	94
5		6	303	>300		94	94
6		6	303	>300		94	94
7		6	303	>300		95	95
8		6	303	>300		95	95
9 <sup>e</sup>		12	303	>300		84	84
10 <sup>ef</sup>							
11 <sup>ef</sup>		48	303	>300		31	82
12 <sup>ef</sup>							
13 <sup>ef</sup>		48	343	>300		55	83
14 <sup>ef</sup>							
15 <sup>ef</sup>		48	343	>300		41	88
16 <sup>ef</sup>		48	303	>300		71	87
17 <sup>ef</sup>							
18 <sup>ef</sup>		48	343	>300		<1	
19 <sup>ef</sup>							
		48	343	>300		13	80
							
		48	343	>300		48 <sup>g</sup>	48 (E/Z=1/4)
							
		48	343	>370		85 <sup>g</sup>	85 (E/Z = 12/1)
							
		48	343	>300		71 <sup>g</sup>	71 (E/Z=1/3)
							
		48	343	>370		85 <sup>g</sup>	85 (E/Z = 11/1)
							

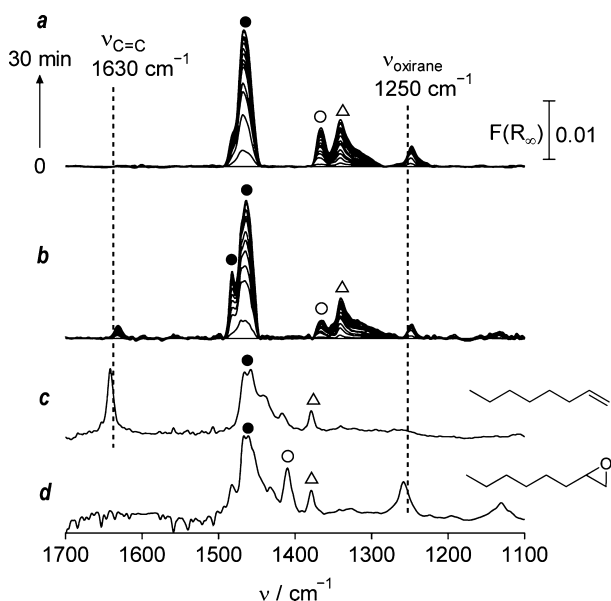
<sup>a</sup>Reaction conditions: TiO<sub>2</sub> (sample 9, 10 mg), substrate (100 μmol), 2-PrOH/MeCN mixture (5/5 v/v, 5 mL), N<sub>2</sub> (1 atm), Xe lamp. <sup>b</sup>Determined by GC. <sup>c</sup>First reuse. <sup>d</sup>Second reuse. <sup>e</sup>Substrate (20 μmol). <sup>f</sup>Catalyst (100 mg). <sup>g</sup>1,2-Diphenylethanol is formed as a byproduct. The yields are 42% (entry 16), 11% (entry 17), 20% (entry 18), and 13% (entry 19), respectively.

phase at 303 K. An absorption band assigned to the C=C stretching vibration ( $\nu_{C=C}$ ) of 1-octene observed at  $\sim 1630$  cm<sup>-1</sup> (Figure 6c) does not appear, although a distinctive  $\nu_{C=C}$  band is observed in the case of styrene oxide (Figure 2a). This suggests that aliphatic epoxides are, indeed, less active than aromatic epoxides. In this case, a vibrational band assigned to a Ti–O–C bond, as often observed at  $\sim 1260$  cm<sup>-1</sup>,<sup>40,41</sup> scarcely appears in the spectra. This suggests that ring-opened intermediates (Scheme 3A.b,c) are scarcely produced during the DRIFT analysis and the electron transfer from Ti<sup>3+</sup> to the oxygen atom of epoxide (oxirane ring-opening, Scheme 3A.a) is the rate-determining step for deoxygenation. The above ab initio calculation and DRIFT analysis indicate that the low reactivity of aliphatic epoxides is ascribed to the low efficiency for the electron transfer from Ti<sup>3+</sup> to the oxygen atoms, which suppresses ring-opening of the oxirane ring (Scheme 3A.a).

For these unreactive aliphatic epoxides, the reaction at elevated temperature is effective. As shown by entries 11 and 13, the reaction at 343 K enhances deoxygenation and affords the corresponding alkenes with moderate yields (55 and 71%).

As shown in Figure 6b, the DRIFT analysis of 1,2-epoxyoctane performed at 343 K shows the  $\nu_{C=C}$  band at  $\sim 1630$  cm<sup>-1</sup>, although at a weak level. This suggests that the electron transfer from Ti<sup>3+</sup> to the oxygen atom of the aliphatic epoxide is, indeed, enhanced at elevated temperature. In contrast, as shown by entries 14 and 15, the internal epoxide exhibits very low reactivity, even at elevated temperature, as also observed in other catalytic system.<sup>10</sup> This is probably due to the steric hindrance by adjacent alkyl chains, which suppresses the electron transfer from Ti<sup>3+</sup> to the oxygen atom of epoxide.

In the case of (*Z*)- and (*E*)-stilbene oxides (entries 16 and 18), the alkene selectivities are very low (48 and 71%) because large amounts of 1,2-diphenylethanol are formed as a byproduct. Several experimental results<sup>42</sup> suggest that the byproduct is produced by photoexcitation of a ring-opened intermediate (Scheme 3A.b) via the absorption of short-wavelength UV light ( $\sim <350$  nm) followed by abstraction of hydrogen atom from 2-PrOH, as is also observed for related diphenylethane derivatives.<sup>43,44</sup> In these cases, photoexcitation of TiO<sub>2</sub> with relatively longer-wavelength light is effective for



**Figure 6.** Time-dependent change in the DRIFT spectra of 1,2-epoxyoctane adsorbed onto TiO<sub>2</sub> (sample 9) in the gas phase at (a) 303 and (b) 343 K. ATR spectra of (c) 1-octene and (d) 1,2-epoxyoctane measured at 303 K. The absorption bands indicated by ●, ○, and △ are assigned to CH<sub>2</sub> scissoring, CH<sub>3</sub> symmetric bending, and CH<sub>2</sub> wagging, respectively (refs 53 and 54).

selective alkene formation. As shown by entries 17 and 19, the reaction of (*Z*)- and (*E*)-stilbene oxides, when performed by the irradiation of >370 nm light, exhibits enhanced alkene selectivity (both 85%).<sup>45,46</sup> These data suggest that reaction temperature and irradiation wavelengths are the most important factors for efficient and selective deoxygenation of unreactive epoxides.

## CONCLUSION

We clarified the mechanism for deoxygenation of epoxides on the photoactivated TiO<sub>2</sub> by means of XPS and DRIFT analysis. This catalytic deoxygenation is facilitated by the combination of electron transfer from surface Ti<sup>3+</sup> atoms on TiO<sub>2</sub> to the oxygen atom of epoxides, promoting deoxygenation of epoxides, and the photocatalytic action of TiO<sub>2</sub>, promoting regeneration of surface Ti<sup>3+</sup> atoms with alcohol as a reducing agent. This photoprocess has significant advantages over the early reported processes: (i) noble-metal-free and inexpensive heterogeneous catalyst (TiO<sub>2</sub>), (ii) safe and inexpensive reducing agent (alcohol), (iii) milder reaction conditions (relatively low temperature (<343 K) and atmospheric pressure). This process, therefore, has a potential to enable green deoxygenation of epoxides. The role of surface Ti<sup>3+</sup> atoms on the photoactivated TiO<sub>2</sub> clarified here may help open a new strategy toward the design of more efficient photocatalysts and the creation of new methods for photocatalysis-based organic synthesis.

## EXPERIMENTAL SECTION

**Photoreaction.** Each respective epoxide was dissolved in a 2-PrOH/MeCN mixture (5/5 v/v, 5 mL). The solution and catalyst were added to a Pyrex glass tube ( $\phi$  12 mm; capacity, 20 mL), and the tube was sealed with a rubber septum cap. The catalyst was dispersed well by ultrasonication for 5 min, and N<sub>2</sub> gas was bubbled through the solution for 5 min. The tube was

immersed in a temperature-controlled water bath (error:  $\pm 0.5$  K),<sup>47</sup> and photoirradiated with magnetic stirring using a 2 kW Xe lamp (USHIO Inc.;  $\lambda > 300$  nm).<sup>48</sup> The intensity of light at 300–450 nm was determined to be 27.3 W m<sup>-2</sup>. In some cases, a grass filter was used to give light wavelength of  $\lambda > 370$  nm, where the intensity of light at 370–450 nm was 12.8 W m<sup>-2</sup>. After the photoreaction, the catalyst was separated by centrifugation, and the resulting solution was analyzed by GC–FID. The substrate and product concentrations were calibrated with authentic samples. Analysis was performed at least three times, and the errors were  $\pm 0.2\%$ .

**Action Spectrum Analysis.** The reaction was carried out using a 2-PrOH/MeCN (5/5 v/v) mixture (2 mL) containing styrene oxide (0.04 mmol) and JRC-TIO-6 TiO<sub>2</sub> (sample 9, 4 mg) within a Pyrex glass tube ( $\phi$  12 mm; capacity, 20 mL). After ultrasonication and N<sub>2</sub> bubbling, the solution was photoirradiated using a 2 kW Xe lamp for 1 h, where the light was monochromated by band-pass glass filters (Asahi Techno Glass Co.).<sup>49</sup> The full-width at half-maximum (fwhm) of the light was 11–16 nm. Apparent intensity of light entered into the reaction vessel was determined with a spectroradiometer USR-40 (USHIO Inc.).<sup>50</sup> The apparent quantum yields ( $\Phi_{\text{AQY}}$ ) for deoxygenation of styrene oxide (two-electron-reduction reduction process) was calculated using the following equation.<sup>51</sup>

$$\Phi_{\text{AQY}} = \frac{[\text{styrene formed } (\mu\text{mol})] \times 2 \times N \times hc}{H \times A \times \lambda \times t} \quad (1)$$

where  $N$  is the Avogadro's number (mol<sup>-1</sup>),  $H$  is the apparent intensity of light entered into the tube (W m<sup>-2</sup>),  $A$  is the absorption cross section of the solution (m<sup>2</sup>),  $h$  is the Planck's constant (J s),  $c$  is the light speed (m s<sup>-1</sup>),  $\lambda$  is the light wavelength (m), and  $t$  is the time for photoirradiation (s), respectively.

**XPS Analysis.** The analysis was performed using a JEOL JPS-9000MX spectrometer with Mg K $\alpha$  radiation as the energy source.<sup>52</sup> Measurements were carried out as follows: TiO<sub>2</sub> (sample 9, 50 mg) was set in a vacuum line and evacuated (0.9 Pa) at 423 K for 3 h. The sample was placed on a sample stage immediately and evacuated at room temperature for 6 h, and measurement was started (Figure 1a). After pretreatment of TiO<sub>2</sub> (0.9 Pa, 423 K, 3 h), styrene oxide (20  $\mu$ mol) was introduced in the gas phase at 303 K, and the cell was left for 30 min. The sample was placed on a sample stage immediately and evacuated at room temperature for 6 h, and measurement was started (Figure 1b). After the measurement, the sample (50 mg) was added to 2-PrOH (10 mL) and photoirradiated for 6 h under N<sub>2</sub> atmosphere in a manner similar to that for photoreaction of epoxide. The resulting powders were recovered by centrifugation and placed on a sample stage immediately. The sample was evacuated at room temperature for 6 h, and measurement was started (Figure 1c).

**DRIFT Analysis.** The spectra were measured on a FT/IR 610 system equipped with a DR-600B in situ cell (Jasco Corp.).<sup>38</sup> TiO<sub>2</sub> (sample 9; 50 mg) was placed in a DR cell and evacuated (0.9 Pa) at 423 K for 3 h. Epoxide (20  $\mu$ mol) was introduced to the cell at 303 K, and measurement was started. Absorption bands in Figure 6 were assigned according to the literature.<sup>53,54</sup>

**Other Analysis.** DR UV–vis spectra were measured on an UV–vis spectrophotometer (Jasco Corp.; V-550 with Integrated Sphere Apparatus ISV-469) with BaSO<sub>4</sub> as a reference. Absorption spectra were measured on an UV–vis photodiode

array spectrophotometer (Shimadzu; Multispec-1500). XRD patterns were obtained by Philips X'Pert-MPD spectrometer.

**Computational Details.** Ab initio calculations were performed at the DFT level within the Gaussian 03 program,<sup>55</sup> using the B3LYP/6-31G(d) basis set. The excited states of respective epoxides were calculated with the time-dependent TD-DFT at the same level of optimization. Cartesian coordinates for the respective epoxides are summarized at the end of the Supporting Information.

## ■ ASSOCIATED CONTENT

### ● Supporting Information

XRD patterns of respective TiO<sub>2</sub> (Figure S1), IR spectrum of polymerized byproduct (Figure S2), DRIFT spectra of nitrobenzene adsorbed onto the respective TiO<sub>2</sub> (Figure S3), interfacial plots of epoxides (Figure S4), absorption spectra of stilbenes (Figure S5), and Cartesian coordinates of epoxides. This material is available free of charge via the Internet at <http://pubs.acs.org>.

## ■ AUTHOR INFORMATION

### Corresponding Author

\*E-mail: [shiraish@cheng.es.osaka-u.ac.jp](mailto:shiraish@cheng.es.osaka-u.ac.jp).

### Notes

The authors declare no competing financial interest.

## ■ ACKNOWLEDGMENTS

This work was supported by a Grant-in-Aid for Scientific Research (No. 23360357) from the Ministry of Education, Culture, Sports, Science and Technology, Japan (MEXT).

## ■ REFERENCES

- Silverman, R. B. *J. Am. Chem. Soc.* **1981**, *103*, 3910–3915.
- Preusch, P. C.; Suttie, J. W. *J. Org. Chem.* **1983**, *48*, 3301–3305.
- Corey, E. J.; Su, W. G. *J. Am. Chem. Soc.* **1987**, *109*, 7534–7536.
- Kraus, G. A.; Thomas, P. J. *J. Org. Chem.* **1988**, *53*, 1395–1397.
- Johnson, W. S.; Plummer, M. S.; Reddy, S. P.; Bartlett, W. R. *J. Am. Chem. Soc.* **1993**, *115*, 515–521.
- Larock, R. C. *Comprehensive Organic Transformations*; Wiley: New York, 1999; p 272.
- Mitsudome, T.; Mikami, Y.; Matoba, M.; Mizugaki, T.; Jitsukawa, K.; Kaneda, K. *Angew. Chem., Int. Ed.* **2012**, *51*, 136–139.
- Mitsudome, T.; Noujima, A.; Mikami, Y.; Mizugaki, T.; Jitsukawa, K.; Kaneda, K. *Angew. Chem., Int. Ed.* **2010**, *49*, 5545–5548.
- Mitsudome, T.; Noujima, A.; Mikami, Y.; Mizugaki, T.; Jitsukawa, K.; Kaneda, K. *Chem.—Eur. J.* **2010**, *16*, 11818–11821.
- Noujima, A.; Mitsudome, T.; Mizugaki, T.; Jitsukawa, K.; Kaneda, K. *Angew. Chem., Int. Ed.* **2011**, *50*, 2986–2989.
- Ni, J.; He, L.; Liu, Y. M.; Cao, Y.; He, H. Y.; Fan, K. N. *Chem. Commun.* **2011**, *47*, 812–814.
- Ke, X.; Sarina, S.; Zhao, J.; Zhang, X.; Chang, J.; Zhu, H. *Chem. Commun.* **2012**, *48*, 3509–3511.
- Ke, X.; Zhang, X.; Zhao, J.; Sarina, S.; Barry, J.; Zhu, H. *Green Chem.* **2013**, *15*, 236–244.
- Li, Y.; Ji, H.; Chen, C.; Ma, W.; Zhao, J. *Angew. Chem., Int. Ed.* **2013**, *52*, 12636–12640.
- Maruska, H. P.; Ghosh, A. K. *Sol. Energy* **1978**, *20*, 443–458.
- RajanBabu, T. V.; Nugent, W. A.; Beattie, M. S. *J. Am. Chem. Soc.* **1990**, *112*, 6408–6409.
- RajanBabu, T. V.; Nugent, W. A. *J. Am. Chem. Soc.* **1994**, *116*, 986–997.
- Gansäuer, A.; Bluhm, H. *Chem. Rev.* **2000**, *100*, 2771–2788.
- Gansäuer, A.; Pierobon, M.; Bluhm, H. *Angew. Chem., Int. Ed.* **1998**, *37*, 101–103.
- Gansäuer, A.; Lauterbach, T.; Narayan, S. *Angew. Chem., Int. Ed.* **2003**, *42*, 5556–5573.
- Justicia, J.; Jiménez, T.; Morcillo, S. P.; Cuerva, J. M.; Oltra, J. E. *Tetrahedron* **2009**, *65*, 10837–10841.
- Papageorgiou, A. C.; Beglitis, N. S.; Pang, C. L.; Teobaldi, G.; Cabailh, G.; Chen, Q.; Fisher, A. J.; Hofer, W. A.; Thornton, G. *Proc. Natl. Acad. Sci. U.S.A.* **2010**, *107*, 2391–2396.
- Rodriguez, J. A.; Jirsak, T.; Liu, G.; Hrbek, J.; Dvorak, J.; Maiti, A. *J. Am. Chem. Soc.* **2001**, *123*, 9597–9605.
- Maldotti, A.; Molinari, A.; Amadelli, R. *Chem. Rev.* **2002**, *102*, 3811–3836.
- Palmisano, G.; Augugliaro, V.; Pagliano, M.; Palmisano, L. *Chem. Commun.* **2007**, 3425–3437.
- Fagnoni, M.; Dondi, D.; Ravelli, D.; Albin, A. *Chem. Rev.* **2007**, *107*, 2725–2756.
- Shiraishi, Y.; Hirai, T. *J. Photochem. Photobiol. C* **2008**, *9*, 157–170.
- Seung, S. L. N.; Young, R. N. *J. Polym. Sci. Polym. Lett. Ed.* **1980**, *18*, 89–96.
- Reiß, S.; Krumm, H.; Niklewski, A.; Staemmler, V.; Wöll, C. *J. Chem. Phys.* **2002**, *116*, 7704–7713.
- Cherian, S.; Wamser, C. C. *J. Phys. Chem. B* **2000**, *104*, 3624–3629.
- Klust, A.; Madix, R. J. *Surf. Sci.* **2006**, *600*, 5025–5040.
- Wei, W.; Huang, W. X.; White, J. M. *Surf. Sci.* **2004**, *572*, 401–408.
- Nyquist, R. A.; Fiedler, S. *Vib. Spectrosc.* **1994**, *7*, 149–162.
- Brinkley, D.; Engel, T. *J. Phys. Chem. B* **1998**, *102*, 7596–7605.
- Panayotov, D. A.; Burrows, S. P.; Morris, J. R. *J. Phys. Chem. C* **2012**, *116*, 4535–4544.
- Wang, X.; Feng, Z.; Shi, J.; Jia, G.; Shen, S.; Zhou, J.; Li, C. *Phys. Chem. Chem. Phys.* **2010**, *12*, 7083–7090.
- Shiraishi, Y.; Togawa, Y.; Tsukamoto, D.; Tanaka, S.; Hirai, T. *ACS Catal.* **2012**, *2*, 2475–2481.
- Shiraishi, Y.; Hirakawa, H.; Togawa, Y.; Sugano, Y.; Ichikawa, S.; Hirai, T. *ACS Catal.* **2013**, *3*, 2318–2326.
- Bessac, F.; Frenking, G. *Inorg. Chem.* **2003**, *42*, 7990–7994.
- Lei, P.; Wang, F.; Zhang, S.; Ding, Y.; Zhao, J.; Yang, M. *ACS Appl. Mater. Interfaces* **2014**, *6*, 2370–2376.
- Lei, P.; Wang, F.; Gao, X.; Ding, Y.; Zhang, S.; Zhao, J.; Liu, S.; Yang, M. *J. Hazard. Mater.* **2012**, 227–228, 185–194.
- The following experimental results were obtained: (1) Photoirradiation (>300 nm) of (Z)- or (E)-stilbene with TiO<sub>2</sub> in the presence of water under N<sub>2</sub> does not promote any reactions; (2) photoirradiation (>300 nm) of (Z)- or (E)-stilbene oxide with TiO<sub>2</sub> under N<sub>2</sub> in the presence of zeolite as a dehydration agent still produces 1,2-diphenylethanol with yields similar to those obtained without zeolite; (3) photoirradiation (>300 nm) of (Z)- or (E)-stilbene oxide with TiO<sub>2</sub> under N<sub>2</sub> produces 1,2-diphenylethanol, even at the initial stage of reaction, and the selectivity scarcely changes with photoirradiation time. These data suggest that the water and stilbenes produced by deoxygenation of stilbene oxides are not involved in the formation of 1,2-diphenylethanol. As reported (refs 43 and 44), photoexcitation of diphenylethane derivatives leads to abstraction of hydrogen atoms from donor molecules, such as alcohols and amines. In the present case, the ring-opened intermediate (Scheme 3A.b) is probably photoexcited by short-wavelength UV light (~<350 nm). Its excited state may lead to abstraction of a hydrogen atom from 2-PrOH, producing 1,2-diphenylethanol.
- Rajesh, C. S.; Givens, R. S.; Wirz, J. *J. Am. Chem. Soc.* **2000**, *122*, 611–618.
- Kandanarachchi, P. H.; Autrey, T.; Franz, J. A. *J. Org. Chem.* **2002**, *67*, 7937–7945.
- As shown in Table 2 (entries 16–19), the selectivity for (Z)- and (E)-stilbenes depends on the irradiation wavelengths. This is due to the photoisomerization of product stilbenes (ref 44). Under >300 nm irradiation conditions, (E)-stilbene exists mainly as a result of the trans-to-cis photoisomerization (entries 16 and 18). In contrast, under >370 nm irradiation conditions (entries 17 and 19), (Z)-stilbene exists

mainly because stilbenes do not absorb light (Figure S5, Supporting Information) and the *Z* form is thermodynamically more stable than the *E* form.

- (46) Arai, T.; Tokumaru, K. *Chem. Rev.* **1993**, *93*, 23–39.
- (47) Tsukamoto, D.; Shiraishi, Y.; Sugano, Y.; Ichikawa, S.; Tanaka, S.; Hirai, T. *J. Am. Chem. Soc.* **2012**, *134*, 6309–6315.
- (48) Shiraishi, Y.; Sugano, Y.; Tanaka, S.; Hirai, T. *Angew. Chem., Int. Ed.* **2010**, *49*, 1656–1660.
- (49) Shiraishi, Y.; Sakamoto, H.; Sugano, Y.; Ichikawa, S.; Hirai, T. *ACS Nano* **2013**, *7*, 9287–9297.
- (50) Sugano, Y.; Shiraishi, Y.; Tsukamoto, D.; Ichikawa, S.; Tanaka, S.; Hirai, T. *Angew. Chem., Int. Ed.* **2013**, *52*, 5295–5299.
- (51) An, X.; Li, K.; Tang, J. *ChemSusChem* **2014**, DOI: 10.1002/cssc.201301194.
- (52) Shiraishi, Y.; Tanaka, K.; Shirakawa, E.; Sugano, Y.; Ichikawa, S.; Tanaka, S.; Hirai, T. *Angew. Chem., Int. Ed.* **2013**, *52*, 8304–8308.
- (53) Limberg, C.; Köppe, R. *Inorg. Chem.* **1999**, *38*, 2106–2116.
- (54) Severcan, F.; Toyran, N.; Kaptan, N.; Turan, B. *Talanta* **2000**, *53*, 55–59.
- (55) Frisch, M. J.; Trucks, G. W.; Schlegel, H. B.; Scuseria, G. E.; Robb, M. A.; Cheeseman, J. R., Jr.; Montgomery, J. A.; Vreven, T.; Kudin, K. N.; Burant, J. C.; Millam, J. M.; Iyengar, S. S.; Tomasi, J.; Barone, V.; Mennucci, B.; Cossi, M.; Scalmani, G.; Rega, N.; Petersson, G. A.; Nakatsuji, H.; Hada, M.; Ehara, M.; Toyota, K.; Fukuda, R.; Hasegawa, J.; Ishida, M.; Nakajima, T.; Honda, Y.; Kitao, O.; Nakai, H.; Klene, M.; Li, X.; Knox, J. E.; Hratchian, H. P.; Cross, J. B.; Bakken, V.; Adamo, C.; Jaramillo, J.; Gomperts, R.; Stratmann, R. E.; Yazyev, O.; Austin, A. J.; Cammi, R.; Pomelli, C.; Ochterski, J. W.; Ayala, P. Y.; Morokuma, K.; Voth, G. A.; Salvador, P.; Dannenberg, J. J.; Zakrzewski, V. G.; Dapprich, S.; Daniels, A. D.; Strain, M. C.; Farkas, O.; Malick, D. K.; Rabuck, A. D.; Raghavachari, K.; Foresman, J. B.; Ortiz, J. V.; Cui, Q.; Baboul, A. G.; Clifford, S.; Cioslowski, J.; Stefanov, B. B.; Liu, G.; Liashenko, A.; Piskorz, P.; Komaromi, I.; Martin, R. L.; Fox, D. J.; Keith, T.; Al-Laham, M. A.; Peng, C. Y.; Nanayakkara, A.; Challacombe, M.; Gill, P. M. W.; Johnson, B.; Chen, W.; Wong, M. W.; Gonzalez, C.; Pople, J. A. *Gaussian 03, revision B.05*; Gaussian, Inc.: Wallingford, CT, 2004.